THE JOURNAL OF PHYSICAL CHEMISTRY C

ARTICLE

pubs.acs.org/JPCC

Photoluminescent Lanthanide-Doped Silica Nanotubes: Sol−Gel Transcription from Functional Template

Yan Qiao, Huanfa Chen, Yiyang Lin, Zhiyi Yang, Xinhao Cheng, and Jianbin Huang*

Beijing National Laboratory for Molecular Sciences (BNLMS), State Key Laboratory for Structural Chemistry of Unstable and Stable Species, College of Chemistry and Molecular Engineering, Peking University, Beijing 100871, China

Supporting Information

ABSTRACT: Functional photoluminescent materials have emerged as a fascinating research subject holding great promise in versatile applications. In this report, photoluminescent lanthanide-organic hybrid nanofibers in hydrogels are fabricated through supramolecular self-assembly, which can serve as functional soft templates to prepare inorganic nanomaterials. By using sol−gel transcription of tetraethylorthosilicate (TEOS), novel lanthanide-doped silica nanotubes are conveniently prepared, in which lanthanide ions are embedded into the silica nanotube walls. In this approach, luminescent lanthanide ions transfer from organic nanofibers into inorganic silica nanotubes. Moreover, different kinds of lanthanide-doped silica nanotubes with tunable photoluminescent emission color can be achieved by changing the doping ions such as Tb^{3+} and co-doping Tb^{3+}/Eu^{3+} in the soft template. The lanthanide-doped silica nanotubes are potentially used as nanostructured optical devices and sensors.

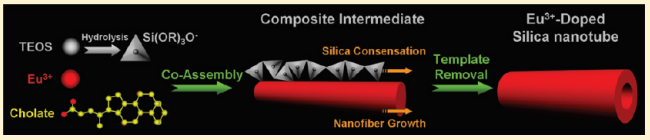

INTRODUCTION

Since the discovery of carbon nanotubes,[1] hollow nanotubes have attracted considerable attention due to their functional significance and potential applications in nanoscale devices, sensors, and energy storage/conversion.[2] In particular, silica nanotubes raise special interest because of their biocompatibility, confined environment as nanocontainers, and feasibility of chemical modification of outer/inner surfaces and edges. Template-directed sol−gel polycondensation of tetraethoxysilane (TEOS) is a representative method to synthesize silica nanomaterials. In the past decade, silica nanotubes as well as nanotube arrays have been fabricated using organogels,[3] hydrogels,[4] carbon nanotubes,[5] and porous alumina membranes with ordered and vertical channel structures[6] as templates. A variety of work have focused on the design of silica nanotubes with different structural parameters, such as size, shape, pore, or wall thickness.[7] Alternatively, the functionalization and application of silica nanotubes are other hot research topics. Particularly, silica nanotubes doped with functional guests have received extensive interests benefiting from the combination of versatile guest functions and high robustness of the silica framework.[8] Shinkai[9] and co-workers utilized a phenanthrolin-appended gelator to create fluorescent silica organic−inorganic composite materials through sol−gel polycondensation. Jung[10] prepared luminescent silica nanotubes with tunable emission colors by cocondensation of different functional dyes and TEOS in a organogel system. In a similar way, metals can be deposited inside the silica wall of rolled paperlike structures templated by a gemini type gelator in the presence of metal salts.[11]

The photoluminescence (PL) properties of trivalent lanthanide ions have aroused tremendous interest because of their broad applications in chemical or biological sensors, medical diagnostics, cell imaging, and thin film devices.[12] The attractive features of lanthanide ions as luminescent materials include linelike emission, high quantum yield, long luminescence lifetime (μs−ms range), high photochemical stability, and low long-term toxicity.[13] The loading of lanthanide ions with host materials can offer the advantages of superior mechanical property, better processability, and thermal stability. Recently, Bünzli[14] reported the synthesis of bare and NH_2-functionalized silica nanoparticles (NPs) embedded with lanthanide binuclear helicate using a water-in-oil microemulsion technique. NH_2-functionalized NPs are conjugated with avidin (NP-avidin) or goat antimouse IgG antibody (NP-IgG) to test them as luminescent biomarkers.

Inspired by the above discussion, we are interested in the design of photoluminecent lanthanide-doped silica nanotubes. The silica backbone can not only serve to protect and stabilize the functional entities inside but also allow its optical properties to be probed from outside due to the chemical inertness and optical transparency of silica. On the basis of previous work of metal-cholate supramolecular self-assembly,[15] we use lanthanide-cholate hybrid hydrogels as templates to synthesize lanthanide-doped silica nanotubes. The sol−gel transcription process is accompanied by the encapsulation of lanthanide ions into silica nanotube walls. The diameter of as-prepared silica nanotubes can be adjusted by changing the temperature in the preparation process. In addition, silica nanotubes with different luminescent color can be tuned by doping different lanthanide ions, such as Tb^{3+}, and co-doping Tb^{3+}/Eu^{3+}, into the soft template. A possible mechanism is proposed to disclose the sol−gel transcription process and lanthanide ions incorporation.

Received: January 18, 2011
Published: March 30, 2011

EXPERIMENTAL SECTION

Materials. Sodium cholate (Alfa Aesar, 99%), tetraethylorthosilicate (TEOS, Sigma-Aldrich, 98%), lanthanide nitrates and other chemicals (A.R. Grade of Beijing Chemical Co.) were used as received.

Preparation of Lanthanide-Cholate Hybrid Hydrogels. The lanthanide-cholate hybrid hydrogels were obtained by directly vortex mixing sodium cholate solution with the desired amount of a concentrated lanthanide nitrates solution (0.1 or 0.5 M). The resulting mixture was equilibrated at the desired temperature in a thermostatted bath at least for 3 days before further analyses. During this period, a uniform self-supporting hydrogel can form.

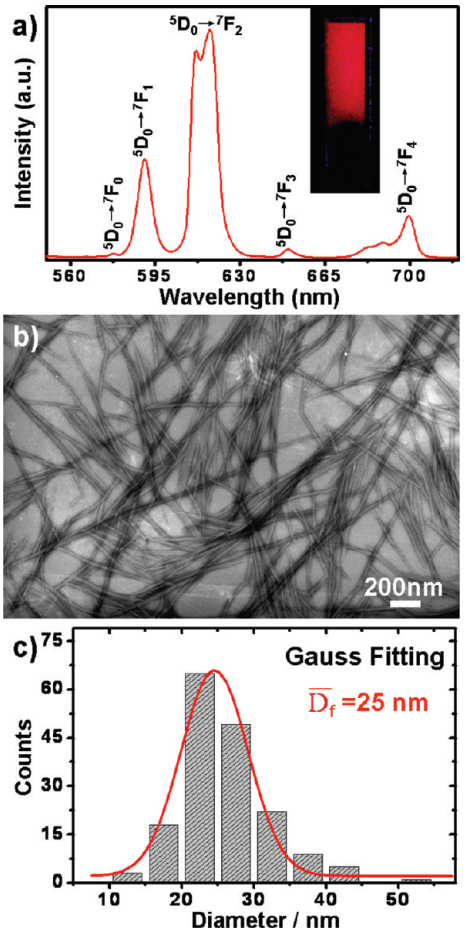

Figure 1. Eu^{3+}-cholate luminescent hydrogels (3.0 mM/1.5 mM) at 25 °C. (a) Emission spectrum (λ_{ex} = 395 nm). The inset shows visual photo under 365 nm illumination (concentration of Eu^{3+}-cholate is 10 mM/30 mM). (b) TEM image of nanofibers. (c) Histogram of the diameter distribution. $\overline{D}_f$ is the average diameter of hydrogel nanofibers.

Preparation of Lanthanide-Doped Silica Nanotubes. In a typical synthesis, 2 mL of sodium cholate solution was incubated at 25 °C for hours. The desired amount of a concentrated lanthanide nitrates solution (0.1 or 0.5 M) was added with intensive vortex. Then, 60 μL of TEOS and 10 μL of ammonia (2 wt %) solution were fed into the test tube. The sample was vortex mixed to ensure complete mixing. Then, the mixture was kept under static conditions in a thermostat container at 25 °C. If not specifically mentioned, the TEOS condensation reaction was performed for 48 h. After the reaction was completed, the hydrogel was totally destroyed, and some floating object was observed in the test tube. The floating object was collected by centrifugation and washed with deionized water three times. Afterward, the products were dried at 40 °C and moved to a furnace to be calcined. The annealing procedure was performed at a heating rate of 5 °C/min and kept at 550 °C for 3 h to remove organic residua. After it was cooled naturally to room temperature, a large quantity of white powder was obtained.

In a control experiment, Eu^{3+}-loaded silica nanotubes were prepared by immersing the bare silica nanotubes into $Eu(NO_3)_3$ solution, and the photoluminescent performance of these nanotubes was investigated. The bare silica nanotubes were synthesized according to previous literature.[4e] Typically, the bare silica nanotubes were immersed into 3 mM $Eu(NO_3)_3$ solution for 48 h, collected by centrifugation, and washed with deionized water for three times. Then, calcinations were carried out at a heating rate of 5 °C/min and kept at 550 °C for 3 h to remove organic residua.

Characterization of Hybrid Hydrogels. A slice of hydrogel was placed on a copper grid and then dried freely under ambient conditions. Then, the nanofibers were characterized by transmission electron microscopy (TEM, JEM-100CX, 100 kV). Photoluminescent measurements were performed on an Edinburgh FLS920 lifetime and steady-state fluorescence spectrophotometer. ζ-Potentials were measured using a temperature-controlled ZetaPALS Zeta Potential Analyzer (Brookhaven Instruments Corp.).

Characterization of Lanthanide-Doped Silica Nanotubes. The obtained nanotubes were characterized by scanning electron microscopy (SEM; Hitachi S4800, 5 kV), TEM (JEOL JEM-100CX, 100 kV), energy-dispersive spectroscopy (EDS; FEI Tecnai F30, 300 kV), and Brunauer–Emmett–Teller (BET; Micromeritics ASAP 2010 system, −196 °C). For the TEM and

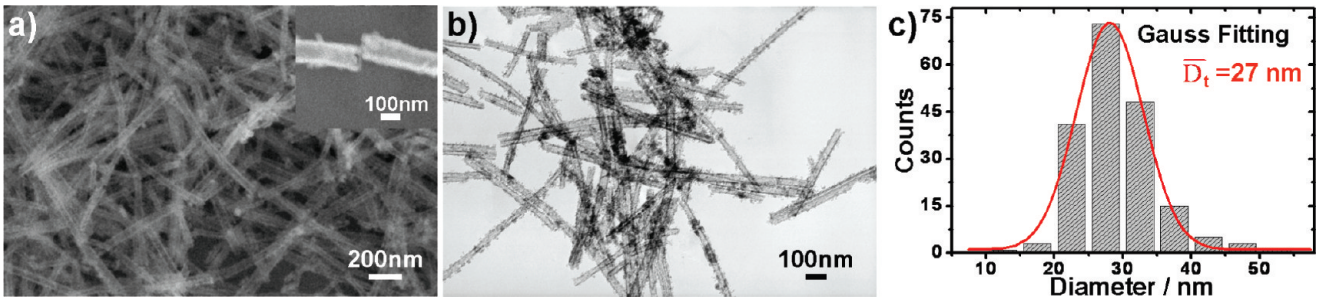

Figure 2. Silica nanotubes that are obtained from Eu^{3+}-cholate hydrogels (3.0 mM/1.5 mM) at 25 °C: (a) FE-SEM image (magnified image insert), (b) TEM image, and (c) histogram of the diameter distribution. $\overline{D}_t$ is the average diameter of silica nanotubes.

SEM measurements, the obtained products were dispersed in water and dropped onto a Formvar-covered copper grid and a silicon wafer, respectively, followed by drying naturally. The steady-state fluorescence spectra were measured with a FLS 920 spectrofluorometer of Edinburgh Instruments using a monochromated Xe lamp as an excitation source. Time-resolved fluorescence spectra measurement were performed with a Lifespec Red spectrofluorometer of Edinburgh Instruments equipped with a Hamamatsu picosecond light pulser C8898 using 393 nm laser with a repetition rate of 1 MHz as a light source. For each measurement, at least 3000 photon counts were collected in the peak channel to ensure the decay quality. The goodness of fit of decay curves, χ^2, was no more than 1.3. For the fluorescence measurements of silica nanotubes, a cell made of quartz glass was used as a solid sample container. For confocal fluorescence microscopy observation, a drop of suspension that contains silica nanotube was placed onto a precleaned glass surface, which was covered by a slide, and then dried naturally. The microstructure observation was conducted on a Nikon $A1_R$-si confocal laser scanning microscope under a filtered 405 nm laser. For nitrogen adsorption and desorption experiments, the samples are degassed at 350 °C overnight under vacuum (10^{-5} Torr) before measurement. The pore size distribution was calculated from the adsorption branch of the isotherm by the Barrett−Joyner−Halenda (BJH) method, and the specific surface area was obtained by the BET method. Each of the results had been repeated three times to give the average values.

RESULTS AND DISCUSSION

Transcription of Europium-Doped Silica Nanotubes from Europium-Cholate Hybrid Hydrogel. As a representative demonstration, the preparation of europium-doped silica nanotubes templated by europium-cholate supramolecular nanofibers is described in detail. As shown in Figure 1a insert, Eu^{3+}-cholate hybrid hydrogel is a red light emitter under UV light irradiation at room temperature. Figure 1a gives the photoluminescent emission spectra of Eu^{3+}-cholate hybrid hydrogel (3.0 mM/1.5 mM). The emission spectrum shows a typical emission of europium ion with significant intensity enhancement. The photoluminescent spectrum consists of a series of lines, which is ascribed to the intra4f^6 $^5D_0 \rightarrow {}^7F_{0-4}$ transitions under direct intra4f^6 excitation (λ_{ex} = 395 nm). The decay curve of $^5D_0$ emission monitored within the $^5D_0 \rightarrow {}^7F_2$ emission line (λ_{em} = 618 nm) under direct intra4f^6 excitation (Figure S1 in the Supporting Information) displays a single exponential behavior. The lifetime value (τ) is calculated to be about 948 μs. The TEM technique without staining reagents is performed to reveal the self-assembled nanostructures in Eu^{3+}-cholate hydrogel. As shown in Figure 1b, well-defined nanofibers with micrometers' length are spontaneously formed in Eu^{3+}-cholate system at 25 °C. The statistical distribution of fiber diameters collected from TEM images shows that the fiber diameters are in the range of 10−55 nm (Figure 1c). The average diameter calculated by Gauss fitting is 25 nm.

In our experiment, TEOS is injected into the Eu^{3+}-cholate mixture at the early stage of fibrous nanostructures growth. This indicates that the processes of organic nanofiber formation and silica polycondensation take place simultaneously. After the hydrolysis and condensation of TEOS with ammonia as a catalyst, silica nanotubes can be obtained. Field emission scanning electron microscopy (FE-SEM; Figure 2a) and TEM (Figure 2b) provide large scale views of massive uniform silica nanotubes that are several micrometers' long. The insert SEM image in Figure 2a clearly shows the broken open end of nanotubes. The diameters of nanotubes are in the range of 10−55 nm, with 27 nm in average as calculated by Gauss fittings (Figure 2c), which is comparable to that of Eu^{3+}-cholate nanofibers. The wall thickness of silica nanotubes is quite thin and uniform (4−6 nm). It is also noticed that the nanotubes are rather rigid, which is consistent with the soft template. The good agreement of structural size and morphology of silica tubes with that of Eu^{3+}-cholate supramolecular nanofibers manifests the successful transcription of soft template into silica nanotubes.

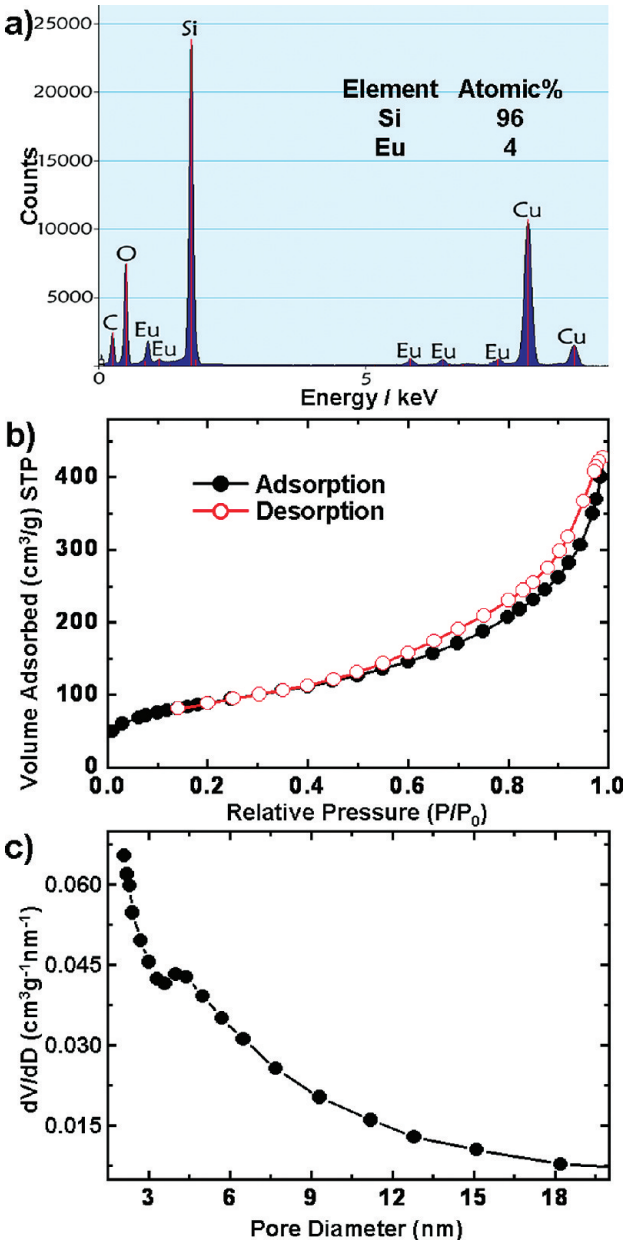

Figure 3. Composition and properties of Eu^{3+}-doped silica nanotubes. (a) EDS result. (b) Nitrogen adsorption−desorption isotherms; STP, standard temperature and pressure. (c) BJH adsorption pore volume distribution curves.

dx.doi.org/10.1021/jp200515s |J. Phys. Chem. C 2011, 115, 7323–7330

The composition of as-prepared silica nanotubes is confirmed by EDS. As shown in the EDS spectra (Figure 3a), the two distinct peaks of silicon and oxygen are observed, indicating that the tubes are composed of silica. The existence of europium peaks reveals the successful doping of europium ions. The atomic ratio of Si/Eu is roughly 96:4. The specific surface areas and pore size distributions of synthetic silica nanotubes are measured by nitrogen adsorption and desorption measurements. The N_2 adsorption−desorption isotherms of the silica nanotubes can be classified into type IV hysteresis loop (Figure 3b), indicating the presence of mesopores on the walls of silica nanotubes. The BET surface area calculated from N_2 adsorption/desorption isotherms is 328 m^2/g. The BJH pore volume and average pore size are 0.65 cm^3/g and 8.2 nm, respectively (Figure 3c).

The PL properties of the as-synthesized silica nanotubes are also investigated. Under irradiation by ultraviolet light, the nanotubes emit strong red light in the dark (Figure 4a insert). The emission spectrum of europium-doped silica nanotubes consists of a series of broadened lines that originates from the intra4f^6 $^5D_0 \rightarrow {}^7F_{0-4}$ transitions of europium ions (Figure 4a). This is similar to the spectrum of Eu^{3+}-cholate nanofibers. The

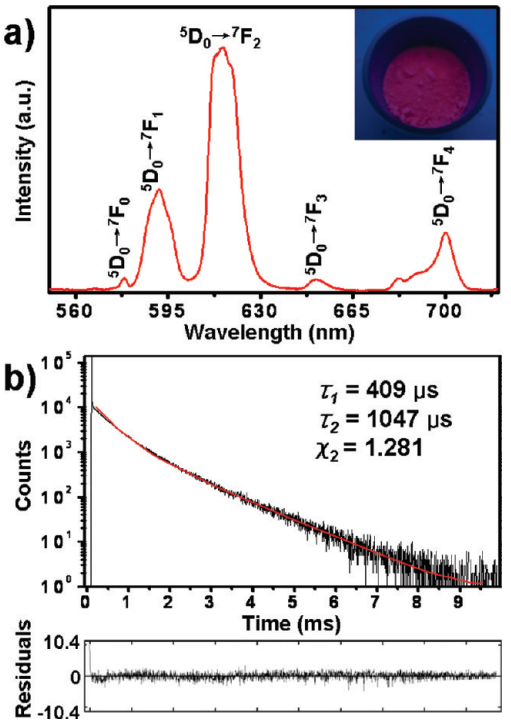

Figure 4. (a) Room temperature emission spectrum (λ_{ex} = 395 nm) and (b) PL decay curve of europium-doped silica nanotubes obtained from Eu^{3+}-cholate hydrogel (3.0 mM/1.5 mM).

$^5D_0$ emission decay curve of silica nanotube (Figure 4b) is monitored within the $^5D_0 \rightarrow {}^7F_2$ emission line under direct intra4f^6 excitation ($^5L_6$, 395 nm). The decay curve displays a double exponential behavior with the lifetime (τ) of 409 and 1047 μs. This indicates the presence of two types of Eu^{3+} local environment, which is on the surface or inside the nanotubes wall.

Confocal fluorescence microscopy is also performed to reveal the luminescence of europium-doped silica nanotubes. The incorporation of europium ion can impart self-indicative advantages to silica nanotubes, in which europium serves as the indicative agents under fluorescence microscopy. Under a filtered 405 nm laser, a large amount of nanotubes with bright red emission (the characteristic emission color of Eu^{3+} ions) can be observed (Figure 5a). The nanotubes extend to tens of micrometers in length. The corresponding bright-field measurement shows that the selected area is bundles of nanotubes in low-magnified observation (Figure 5b). The overlay of confocal luminescence images and bright-field images demonstrates the observed luminescence originates from silica nanotubes.

Europium-Doped Silica Nanotubes with Tunable Diameter. It is noteworthy that the structural parameter of self-assembled europium-cholate nanofibers can be tuned by facilely varying temperature. For example, the supramolecular fibers have the diameters of 5−45 nm at 15 °C and 15−65 nm at 60 °C (Figure 6a,d). The corresponding histograms of diameter distribution are provided in Figure 6c,f. The average diameter analyzed by Gauss fitting increases, and the mean diameters are about 15 and 32 nm, respectively. Considering the tunability in size, these fibers are supposed to be promising templates to synthesize size-tunable nanomaterials by controlling thermal conditions. According to this idea, TEOS and europium nitrate are added to sodium cholate samples at the incubation temperatures of 15 and 60 °C. As expected, silica nanotubes with different diameters are prepared (Figure 6b,e). At 15 °C, silica nanotubes with the diameters of 5−30 nm (15 nm in average) are obtained. At 60 °C, the diameters of silica nanotubes are in the range of 15−45 nm (33 nm in average). It seems that the diameter of as-synthesized silica nanotube increases under higher temperature. This result coincides with that of europium-cholate nanofibers.

Explore the Mechanism of Sol−Gel Transcription. To reveal the formation mechanism of europium ion-doped silica nanotubes, further experiments have been done. First, the europium ion concentration is varied to investigate the effect of europium concentration on the transcription performance of Eu^{3+}-cholate template. The concentration of sodium cholate is fixed to 1.5 mM. As shown in Figure 7, when the europium ion concentration is 0.5 mM, only a small amount of silica nanotubes are acquired with tubular morphology (Figure 7a). With the

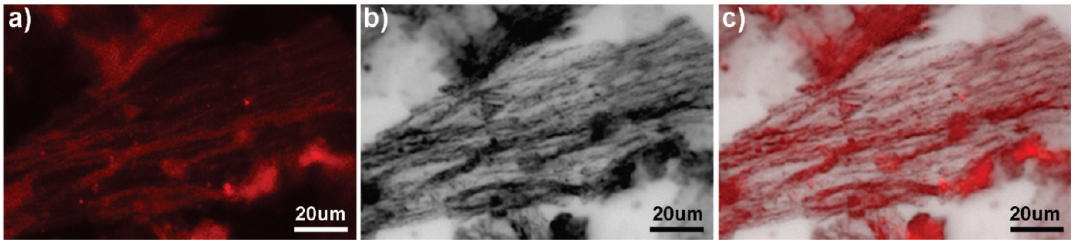

Figure 5. Confocal fluorescence microscopy images of silica nanotubes that are obtained from Eu^{3+}-cholate hydrogels (3.0 mM/1.5 mM) at 25 °C: (a) luminescence images, (b) bright-field optical image, (c) overlay image of both panels a and b.

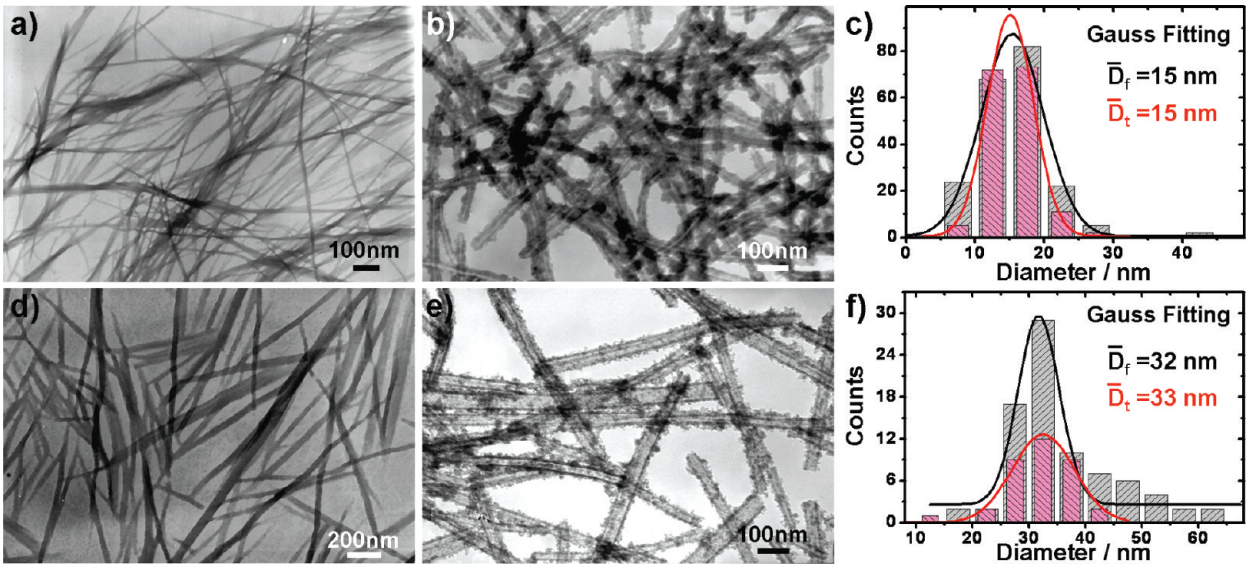

Figure 6. Europium-cholate supramolecular nanofibers incubated at (a) 15 °C and (b) 60 °C and as-prepared europium-doped silica nanotubes: (d) 15 °C and (e) 60 °C. The corresponding diameter statics are shown in panels c and f. The gray columns are donated to nanofiber, and pink ones are indicated silica nanotubes. $\bar{D}_f$ and $\bar{D}_t$ are the average diameter of hydrogel nanofibers and silica nanotubes, respectively.

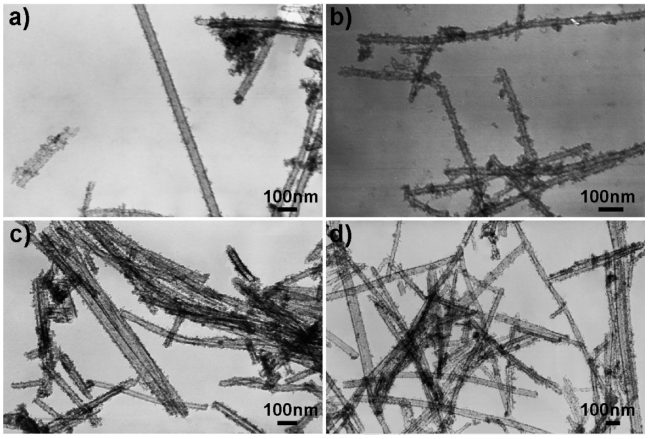

Figure 7. Silica nanotubes prepared at 25 °C with different europium/cholate concentrations: (a) 0.5 mM/1.5 mM, (b) 1.5 mM/1.5 mM, (c) 4.5 mM/1.5 mM, and (d) 6.0 mM/1.5 mM.

increase of europium concentration to 1.5 mM, the as-prepared silica nanotubes are in a higher production and more regular morphology. As the concentration of europium ions exceeds 3.0 mM, massive uniform nanotubes can be obtained. It seems that the Eu^{3+}-cholate nanofibers with higher europium ions concentrations are more efficient at producing silica nanotubes. ζ-Potential measurements are carried out to investigate the surface charge of Eu^{3+}-cholate nanofibers. As Figure 8 shows, the ζ-potential is about −5 mV at 0.5 mM europium ion, indicating that the fibers are slightly negative charged. As the concentration of europium ion increase to 1.5 mM, the nanofibers turn into slightly positively charged with the ζ-potential of 2 mV. A further increase of europium ion concentrations to 3.0, 4.5, and 6.0 mM increases the ζ-potential to about 11 mV. It has been admitted that base-catalyzed hydrolysis of TEOS involves the nucleophilic attack on the silicon atom by the hydroxide anion to form a negatively charged pentacoordinated intermediate, followed by the elimination of an alkoxide

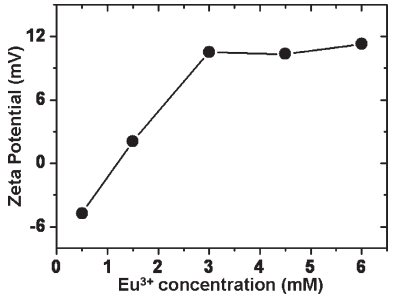

Figure 8. ζ-Potential of Eu^{3+}-cholate nanofibers at different concentrations. The concentration of sodium cholate is 1.5 mM.

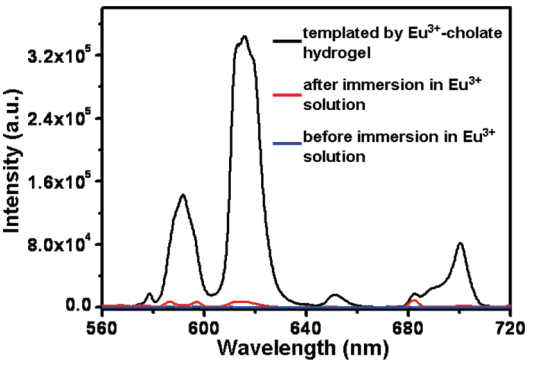

Figure 9. Room temperature emission spectra of silica nanotubes templated by Eu^{3+}-cholate hydrogel, silica nanotubes after immersion in $Eu(NO_3)_3$ solution, and silica nanotubes before immersion in $Eu(NO_3)_3$ solution (λ_{ex} = 395 nm).

anion.[11] The strong intermolecular interactions, that is, electrostatic forces are required to adsorb "anionic" inorganic precursor onto the organic molecular assemblies. Therefore, positive nanofibers can facilitate TEOS hydrolysis and condensation onto nanofiber surface.

dx.doi.org/10.1021/jp200515s |J. Phys. Chem. C 2011, 115, 7323–7330

Scheme 1. Possible Mechanism of SiO_2 Nanotubes Formation in the System of Europium-Cholate Supramolecular Nanofibers

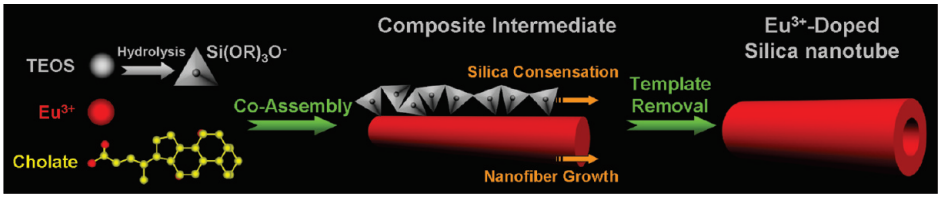

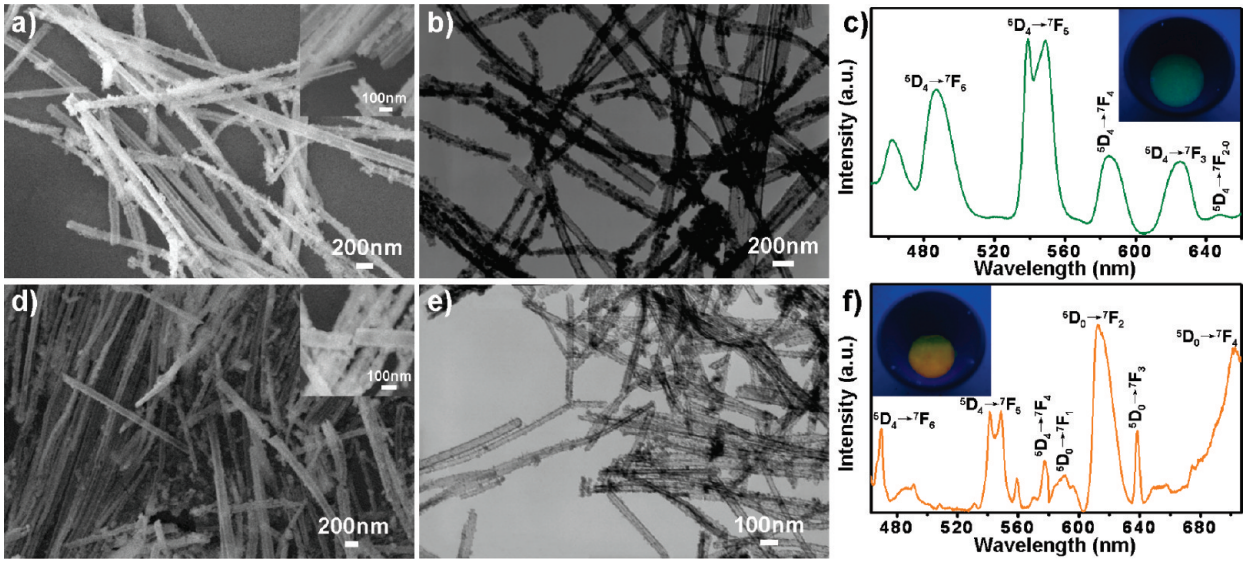

Figure 10. Silica nanotubes that are obtained from Tb^{3+}-cholate (3.0 mM/1.5 mM) hydrogel (a–c) and Tb^{3+}/Eu^{3+}-cholate (3.0 mM/1.5 mM, Tb^{3+}/Eu^{3+} = 99/1) hydrogel (d–f). FE-SEM images (a and d), TEM images (b and e), and room temperature emission spectra (c and f) of the silica nanotubes (λ_{ex} = 370 nm).

Second, it is interesting that europium ions are efficiently uptaken by silica nanotubes. In a control experiment, we immerse the as-prepared silica nanotubes[4e] into 3 mM $Eu(NO_3)_3$ solution for 48 h for doping this nanotube with Eu^{3+}. During the period of immersion, the lanthanide ions are supposed to adsorb onto the surface and pores of silica nanotubes. Then, the silica nanotubes are separated by centrifugation and washed with deioned water. The PL performance of these nanotubes is compared with that of europium-doped nanotubes prepared from europium-cholate hydrogel. As shown in Figure 9, the PL of latter silica nanotubes is more than 50-fold stronger than those prepared by immersion. This means the efficient uptake of Eu^{3+} by silica nanotubes (prepared from europium-cholate hydrogel) is not caused by adsorbing Eu^{3+} on nanotube surface. On the other hand, the leakage of europium ions from the europium-doped silica nanotubes is measured. It is shown that PL of silica nanotubes almost keeps constant when exposed to water, suggesting that the uptake of Eu^{3+} is rather stable. On the basis of the above discussion, Eu^{3+} is supposed to interact strongly with silica network surfaces or be incorporated into the walls of silica nanotubes. In contrast, the Eu^{3+} adsorbing on the surface of silica nanotubes is not stable and may be easily removed by washing.

Third, it is found that silica precursor TEOS should be added into Eu^{3+}-cholate mixture before the hydrogel (template) is formed. In a control experiment, TEOS is added to a preformed Eu^{3+}-cholate hydrogel. It is found that the yield of resultant silica nanotubes is extremely low and the nanotube morphology is in poor uniformity. This is quite different from the traditional soft template mechanism (or post-transcription), in which the TEOS polycondensation reaction is performed on the existing soft template. The failure of traditional soft template mechanism may be explained as follows: (1) TEOS is hydrophobic and hardly soluble in water, and (2) sodium cholate is a facial amphiphile that can solubilize and disperse TEOS in water, while Eu^{3+}-cholate hydrogel is not efficient to disperse TEOS.

In combination with the foregoing results, we now propose a possible co-assembly mechanism for the preparation of photoluminescent silica nanotubes (Scheme 1), which involves three steps: (1) Sodium cholate, europium ion, silica precursor (TEOS), and catalyst are dispersed in water. Hydrophobic TEOS is solubilized by amphiphilic sodium cholate and subsequently hydrolyzes into anionic oligomeric silica species in the presence of ammonia. (2) Eu^{3+}-cholate supramolecular nanofibers are formed driven by hydrophobic effects, hydrogen bonding, and metal coordination.[13] The excessive europium ions make the fibers positively charged, and consequently, the anionic silica oligomers adsorb onto the nanofiber surface through electrostatic attraction. Hence, europium ions, sodium cholate, and anionic oligomeric silica species co-assemble into an organic–inorganic composite intermediate. With the proceeding of silica polycondensation, silica nanotubes networks are formed. During this process, europium ions are supposed to coordinate with silicate groups and co-assemble into the silica nanotubes.

(3) With the entry of Eu^{3+} into silicate networks, the preformed Eu^{3+}-cholate nanofibers as well as hydrogels are destroyed. The final products are obtained after the organic template is removed by washing and calcination.

Preparation of Lanthanide-Doped Silica Nanotubes with Tunable Emission Colors. Benefiting from the universal formation of lanthanide-cholate nanofibers, different kinds of photoluminescent silica nanotubes with tunable emission colors can be obtained by doping different lanthanide ions. For example, the Tb^{3+}-cholate nanofiber presented in Figure S2 in the Supporting Information is a good template to produce Tb^{3+}-doped silica nanotubes. SEM and TEM images shown in Figure 10a,b give convinced evidence of massive uniform nanotubes. The corresponding EDS in Figure S3 in the Supporting Information demonstrates that the molar ratio of Si/Tb is about 95/5. The Tb^{3+}-dopted silica nanotubes shows green light emission under UV light excitation at room temperature (Figure 10c inset). The photoluminescent spectrum displays a series of straight lines ascribed to the intra$^4f_8$ $^5D_4 \rightarrow {}^7F_{6-0}$ transitions of terbium ions (Figure 10c). Moreover, the PL color of silica nanotubes can also be adjusted by co-doping multiple lanthanide ions, such as mixing-up of Tb^{3+}/Eu^{3+} (Figure 10d,e). As shown in the inset of Figure 10f, the silica nanotubes with bisque photoluminescent emission can be designed in the Tb^{3+}/Eu^{3+}-cholate system (Tb^{3+}/Eu^{3+} = 99/1). The characteristic emissions from Tb^{3+} and Eu^{3+} are detected in photoluminescent spectrum, which is excited by 370 nm light. It is interesting that the photoluminescent property can be further adjusted by changing the excitation wavelength. For example, under 395 nm excitation, the Tb^{3+} emission is suppressed (Figure S4 in the Supporting Information), and the silica nanotubes with pink color can be obtained. It is also anticipated that silica nanotubes with different luminescent colors are available by changing the Tb^{3+}/Eu^{3+} ratio.

CONCLUSION

In conclusion, photoluminescent hybrid nanofibers and hydrogels are fabricated through lanthanide-cholate supramolecular self-assembly, which can serve as functional templates to prepare inorganic nanomaterials. Novel lanthanide-doped silica nanotubes are conveniently prepared through sol−gel transcription of TEOS by using lanthanide-cholate nanofibers as templates. It is found that lanthanide ions are efficiently uptaken by silica nanotubes, which makes the nanotubes photoluminescent. A co-assembly mechanism is put forward to describe the formation process of lanthanide-doped nanotubes. Furthermore, the diameter of silica nanotubes can be varied by adjusting environmental temperature. Different kinds of lanthanide-doped silica nanotubes with tunable photoluminescent emission colors can be achieved by changing the doping ions or co-doping of multiple ions in soft templates. The photoluminescent nanotubes are expected to broaden potential applications in optics, sensing, and biomedical engineering.

ASSOCIATED CONTENT

Supporting Information. Photoluminescent study of Eu^{3+}-cholate hybrid hydrogel, TEM image of Tb^{3+}-cholate nanofibers, EDS result of Tb^{3+}-doped silica nanotubes, and photoluminescent study of Tb^{3+}/Eu^{3+}-doped silica nanotubes. This material is available free of charge via the Internet at http://pubs.acs.org.

AUTHOR INFORMATION

Corresponding Author

*Tel: 86-10-62753557. Fax: 86-10-62751708. E-mail: jbhuang@pku.edu.cn.

ACKNOWLEDGMENT

This work was supported by National Natural Science Foundation of China (20873001, 50821061, and 21073006) and National Basic Research Program of China (Grant No. 2007CB936201).

REFERENCES

(1) Iijima, S. *Nature* **1991**, *354*, 56.

(2) (a) Sun, L.; Banhart, F.; Krasheninnikov, A. V.; Rodriguez-Manzo, J. A.; Terrones, M.; Ajayan, P. M. *Science* **2006**, *312*, 1199. (b) Normile, D. *Science* **1999**, *286*, 2056. (c) Hasobe, T.; Fukuzumi, S.; Kamat, P. V. *Angew. Chem., Int. Ed.* **2006**, *45*, 755. (d) Tokudome, H.; Miyauchi, M. *Angew. Chem., Int. Ed.* **2005**, *44*, 1974. (e) Lee, S. B.; Mitcell, D. T.; Trofin, L.; Nevanen, T. K.; Soderlund, H.; Martin, C. R. *Science* **2002**, *296*, 2198. (f) Xing, Y. J.; Xi, Z. H.; Xue, Z. Q.; Zhang, X. D.; Song, J. H.; Wang, R. M.; Xu, J.; Song, Y.; Zhang, S. L.; Yu, D. P. *Appl. Phys. Lett.* **2003**, *83*, 1689. (g) Chen, J.; Xu, L. N.; Li, W. Y.; Gou, X. L. *Adv. Mater.* **2005**, *17*, 582. (h) Che, G. L.; Lakshmi, B. B.; Fisher, E. R.; Martin, C. R. *Nature* **1999**, *393*, 346.

(3) For papers, see the following:(a) Ono, Y.; Nakashima, K.; Sano, M.; Kanekiyo, Y.; Inoue, K.; Hojo, J.; Shinkai, S. *Chem. Commun.* **1998**, 1477. (b) Jung, J. H.; Ono, Y.; Shinkai, S. *Langmuir* **2000**, *16*, 1643. (c) Clavier, G. M.; Pozzo, J. L.; Bouas-Laurent, H.; Liere, C.; Roux, C.; Sanchez, C. *J. Mater. Chem.* **2000**, *10*, 1725. (d) Jung, J. H.; Ono, Y.; Shinkai, S. *Chem.—Eur. J.* **2000**, *6*, 4552. (e) Huang, X.; Weiss, R. G. *Langmuir* **2006**, *22*, 8542. (f) Huang, X.; Weiss, R. G. *Tetrahedron* **2007**, *63*, 7375. (g) For recent reviews, see the following:Llusar, M.; Sanchez, C. *Chem. Mater.* **2008**, *20*, 782. (h) Patzke, G. R.; Krumeich, F.; Nesper, R. *Angew. Chem., Int. Ed.* **2002**, *41*, 2446. (i) Jung, J. H.; Parka, M.; Shinkai, S. *Chem. Soc. Rev.* **2010**, *39*, 4286. (j) van Bommel, K. J. C.; Friggeri, A.; Shinkai, S. *Angew. Chem., Int. Ed.* **2003**, *42*, 980 and references therein. (k) Xue, P. C.; Lu, R.; Li, D. M.; Jin, M.; Bao, C. Y.; Zhao, Y. Y.; Wang, Z. M. *Chem. Mater.* **2004**, *16*, 3702.

(4) (a) Gundiah, G.; Mukhopadhyay, S.; Tumkurkar, U. G.; Govindaraj, A.; Maitra, U.; Rao, C. N. R. *J. Mater. Chem.* **2003**, *13*, 2118. (b) Dickerson, M. B.; Sandhage, K. H.; Naik, R. R. *Chem. Rev.* **2008**, *108*, 4935. (c) Delclos, T.; Aimé, C.; Pouget, E.; Brizard, A.; Huc, I.; Delville, M.-H.; Oda, R. *Nano Lett.* **2008**, *8*, 1929. (d) Pouget, E.; Dujardin, E.; Cavalifer, A.; Moreac, A.; Valéry, C.; Marchi-Artzner, V.; Weiss, T.; Renault, A.; Paternostre, M.; Artzner, F. *Nat. Mater.* **2007**, *6*, 434. (e) Lin, Y. Y.; Qiao, Y.; Gao, C.; Tang, P. F.; Liu, Y.; Li, Z. B.; Yan, Y.; Huang, J. B. *Chem. Mater.* **2010**, *22*, 6711. (f) Jung, J. H.; Shinkai, S.; Shimizu, T. *Nano Lett.* **2002**, *2*, 17. (g) Jung, J. H.; Yoshida, K.; Shimizu, T. *Langmuir* **2002**, *18*, 8724. (h) Yuwono, V. M.; Hartgerink, J. D. *Langmuir* **2007**, *23*, 5033.

(5) (a) Satishkumar, B. C.; Govindaraj, A.; Nath, M.; Rao, C. N. R. *J. Mater. Chem.* **2000**, *10*, 2115. (b) Caruso, R. A.; Antonietti, M. *Chem. Mater.* **2001**, *13*, 3272. (c) Rao, C. N. R.; Nath, M. *J. Chem. Soc., Dalton Trans.* **2003**, 1.

(6) (a) Wang, Z. L.; Gao, R. P.; Jole, J. L.; Stout, J. D. *Adv. Mater.* **2000**, *12*, 1938. (b) Fan, R.; Wu, Y. Y.; Li, D. Y.; Yue, M.; Majumdar, A.; Yang, P. D. *J. Am. Chem. Soc.* **2003**, *125*, 5254. (c) Xu, D. S.; Yu, Y. X.; Miao, Z.; Guo, G. L.; Tang, Y. Q. *Electrochem. Commun.* **2003**, *5*, 673.

(7) (a) Jung, J. H.; Ono, Y.; Shinkai, S. *Angew. Chem., Int. Ed.* **2000**, *39*, 1862. (b) Jung, J. H.; Ono, Y.; Hanabusa, K.; Shinkai, S. *J. Am. Chem. Soc.* **2000**, *122*, 5008. (c) Yang, Y.; Suzuki, M.; Owa, S.; Shirai, H.; Hanabusa, K. *J. Mater. Chem.* **2006**, *16*, 1644. (d) Yang, Y. G.; Suzuki, M.; Owa, S.; Shirai, H.; Hanabusa, K. *Chem. Commun.* **2005**, 4462. (e) Yang, Y. G.; Suzuki, M.; Fukui, H.; Shirai, H.; Hanabusa, K. *Chem. Mater.* **2006**,

18, 1324. (f) Zhang, H.-F.; Wang, C.-M.; Buck, E. C.; Wang, L.-S. *Nano Lett.* **2003**, *3*, 577. (g) Zymunt, J.; Krumeich, F.; Nesper, R. *Adv. Mater.* **2003**, *15*, 1538. (h) Che, S.; Liu, Z.; Ohsuna, T.; Sakamoto, K.; Terasaki, O.; Tatsumi, T. *Nature* **2004**, *429*, 281. (i) Miyaji, F.; Davis, S. A.; Charmant, J. P. H.; Mann, S. *Chem. Mater.* **1999**, *11*, 3021. (j) Seddon, A. M.; Patel, H. M.; Burkett, S. L.; Mann, S. *Angew. Chem., Int. Ed.* **2002**, *41*, 988. (k) Holmstrom, S. C.; King, P. J. S.; Ryadnov, M. G.; Butler, M. F.; Mann, S.; Woolfson, D. N. *Langmuir* **2008**, *24*, 1177. (l) Wang, F. K.; Li, D.; Mao, C. B. *Adv. Funct. Mater.* **2008**, *18*, 4007. (m) Harada, M.; Adachi, M. *Adv. Mater.* **2000**, *12*, 839. (n) Jin, C. Y.; Qiu, H. B.; Han, L.; Shu, M. H.; Che, S. A. *Chem. Commun.* **2009**, 3407.

(8) (a) Fan, H.; Lu, Y.; Stump, A.; Reed, S. T.; Baer, T.; Schunk, R.; Perez-Luna, V.; López, G. P.; Brinker, C. J. *Nature* **2000**, *405*, 56. (b) Li, L.-L.; Fang, C.-J.; Sun, H.; Yan, C.-H. *Chem. Mater.* **2008**, *20*, 5977. (c) Liu, N.; Chen, Z.; Dunphy, D. R.; Jiang, Y.; Assink, R. A.; Brinker, C. J. *Angew. Chem., Int. Ed.* **2003**, *42*, 1731. (d) Liu, N.; Dunphy, D. R.; Atanassov, P.; Bunge, S. D.; Chen, Z.; López, G. P.; Boyle, T. J.; Brinker, C. J. *Nano Lett.* **2004**, *4*, 551. (e) Marlow, F.; McGehee, M. D.; Zhao, D.; Chmelka, B. F.; Stucky, G. D. *Adv. Mater.* **1999**, *11*, 632. (f) Wang, J. F.; Stucky, G. D. *Adv. Funct. Mater.* **2004**, *14*, 409. (g) Okamoto, K.; Shook, C. J.; Bivona, L.; Lee, S. B.; English, D. S. *Nano Lett.* **2004**, *4*, 233.

(9) Fujita, K. S. N.; Shinkai, S. *J. Mater. Chem.* **2005**, *15*, 2747.

(10) Han, W. S.; Kang, Y.; Lee, S. J.; Lee, H.; Do, Y.; Lee, Y.-A.; Jung, J. H. *J. Phys. Chem. B* **2005**, *109*, 20661.

(11) Jung, J. H.; Shinkai, S. *J. Chem. Soc., Perkin Trans. 2* **2000**, 2393.

(12) (a) Binnemans, K. *Chem. Rev.* **2009**, *109*, 4283. (b) Bottrill, M.; Kwok, L.; Long, N. J. *Chem. Soc. Rev.* **2006**, *35*, 557. (c) dos Santos, C. M. G.; Harte, A. J.; Quinn, S. J.; Gunnlaugsson, T. *Coord. Chem. Rev.* **2008**, *252*, 2512. (d) Yu, J. H.; Parker, D.; Pal, R.; Poole, R. A.; Cann, M. J. *J. Am. Chem. Soc.* **2006**, *128*, 2294. (e) Shao, G. S.; Han, R. C.; Ma, Y.; Tang, M. X.; Xue, F. X.; Sha, Y. L.; Wang, Y. *Chem.—Eur. J.* **2010**, *16*, 8647. (f) Song, C. H.; Ye, Z. Q.; Wang, G. L.; Yuan, J. L.; Guan, Y. F. *Chem.—Eur. J.* **2010**, *16*, 6464. (g) Deiters, E.; Song, B.; Chauvin, A.-S.; Vandevyver, C. D. B.; Gumy, F.; Bünzli, J.-C. G. *Chem.—Eur. J.* **2009**, *15*, 885.

(13) (a) Bünzli, J.-C. G.; Piguet, C. *Chem. Soc. Rev.* **2005**, *34*, 1048. (b) Bünzli, J.-C. G. *Acc. Chem. Res.* **2006**, *39*, 53.

(14) Eliseeva, S. V.; Song, B.; Vandevyver, C. D. B.; Chauvin, A.-S.; Wacker, J. B.; Bünzli, J.-C. G. *New J. Chem.* **2010**, *34*, 2915.

(15) (a) Qiao, Y.; Lin, Y. Y.; Wang, Y. J.; Yang, Z. Y.; Liu, J.; Zhou, J.; Yan, Y.; Huang, J. B. *Nano Lett.* **2009**, *9*, 4500. (b) Qiao, Y.; Lin, Y. Y.; Yang, Z. Y.; Chen, H. F.; Zhang, S. F.; Yan, Y.; Huang, J. B. *J. Phys. Chem. B* **2010**, *114*, 11725. (c) Qiao, Y.; Wang, Y. J.; Yang, Z. Y.; Lin, Y. Y.; Huang, J. B. *Chem. Mater.*, **2011**, *23*, 1182.(d) Qiao, Y.; Lin, Y. Y.; Zhang, S. F.; Huang, J. B. *Chem. Eur. J.*, DOI: 10.1002/chem.201003255.